15

# Quantitative local elemental composition analysis of the of materials by EELS technique in STEM under conditions of core-loss lines overlapping

© K.E. Prikhodko,[1,2] M.M. Dement'eva[1]

[1]National Research Center „Kurchatov Institute“,
123182 Moscow, Russia
[2]National Research Nuclear University „MEPhI“,
115409 Moscow, Russia
e-mail: prihodko_ke@nrcki.ru

*Received April 15, 2024*
*Revised April 15, 2024*
*Accepted April 15, 2024*

A method has been developed for processing spectra of characteristic electron energy losses for quantitative analysis of atomic concentrations of elements within the framework of STEM in conditions of close proximity of lines of various elements. In addition, the case of the presence of features on the spectra of energy losses is considered, which, in turn, makes it difficult to isolate the background within the framework of a standard analysis. Using the example of the study of the atomic composition of a thin NbN film, it is shown that the dispersion of the obtained concentration values for various points of the sample is reduced to several atomic percent.

**Keywords:** Characteristic electron energy loss spectroscopy (EELS), transmission scanning electron microscopy (STEM), high-resolution transmission electron microscopy, NbN thin superconducting films, background subtraction in EELS, overlapping of characteristic loss lines.

DOI: 10.61011/TP.2024.08.59009.122-24

## Introduction

Currently developed nanomaterials with desired configurations of performance characteristics are objects of material science design, since the physical properties of nanoelements are determined by both atomic composition and microstructure. Therefore, methods of local verification of atomic composition are extremely relevant, which can be implemented within the framework of transmission scanning electron microscopy (STEM) using the electron energy loss spectroscopy (EELS).

EELS in the field of TEM is by far one of the most informative tools for material studies. This method allows solving a wide range of tasks, in particular, obtaining data on the chemical composition of samples, including the content of light elements and gases H2 and He (core-loss spectroscopy) [1–4]; mapping of the fine structure of spectra, providing information about the local environment of atoms and chemical bonds, the density of DOS states (ELNES — Energy Loss Near Edge Structure) [5–9]; building of the element distribution maps (EELS mapping) [10,11]; construction of filtered images in TEM mode (EFTEM imaging) [12–14]; measurement of plasmon oscillation energy (Low-loss spectroscopy) [15], etc.

The electron probe is focused in a point of small diameter ($\sim 0.1-0.15$ nm) in the STEM mode, which, taking into account the small thickness of the sample ($10-20$ nm) and significant electron energy ($200-300$ keV) allows obtaining analytical information, for example, EELS spectra from an area comparable to the diameter of an electronic probe. The developed standard methods for determining the atomic concentrations of elements at the point of interest of the sample from EELS spectra [16] provide good results when the absorption edges of the analyzed chemical elements are sufficiently separated in energy, i.e., in case of registration of the intensity of the absorption signal, the lines of other elements do not interfere with calculation of the corresponding background curves and integration of the absorption curves in the specified energy intervals.

However, unfortunately, this is not always the case. A typical situation is the imposition of either the absorption edges of various elements themselves, or peaks of the extended structure of the absorption edges of other elements on the absorption edge of the measured element of interest, which increases the error and makes the use of standard procedures ineffective.

Methods known from the literature to overcome this difficulty [17], the essence of which boils down to using reference spectra obtained from „interfering“ elements, and fitting experimental curves to the sum of spectra from all elements using iterative algorithms to find weighting coefficients, are in most cases poorly applicable, since the shape of the absorption line and its intensity, as well as chemical energy shifts, significantly depend on the electronic configuration of interatomic bonds in a chemical compound, its degree of oxidation, as well as on the nearest neighbors for a given atom.

The method of successive transformations of the energy loss spectrum sections developed by the authors is described in this paper on the example of determination of the atomic composition of thin-film niobium nitride on cross-sectional samples, in the spectra of which the niobium absorption

peaks ($Nb-M_{3,2}$) are superimposed on the nitrogen absorption edge ($N-K$),which makes it possible to exclude the impact of the $Nb-M_{3,2}$ absorption lines on the $N-K$ absorption line. This approach has significantly improved the accuracy of measurements of atomic concentrations of elements.

## 1. Experimental method

### 1.1. Microscope and EELS spectrometer

All STEM studies were performed using transmission electron microscope FEI„Titan 80-300ST“ with an electron energy of 200 keV, with a field emission electron source (Schottky FEG) provided with an energy loss spectrometer Gatan„GIF-2001“. The conditions for recording the EELS spectra in transmission scanning mode were selected based on the technical parameters for this microscope and ensuring the registration of the maximum number of electrons that have undergone inelastic scattering. Since one of the defining characteristics of the microscope operation in the STEM mode is the size of the probe, the optimal convergence angle $\alpha$ was 10 mrad, which ensures a minimal contribution of spherical aberrations. The next important parameter affecting the efficiency of electron collection is the receiving angle of the spectrometer $\beta$. The collection angle $\beta$ depends on the type of microscope and is determined by the distance from the screen plane to the plane of the input aperture of the spectrometer, the diameter of the aperture, as well as the length of the camera used. The dependence of the angle $\beta$ on the microscope camera length can be used to select the optimal angle $\beta$ considering all the characteristics of the instrument. The spectra of characteristic electron energy losses in the high-loss region were recorded in this study with a spectrometer input aperture of 3 mm, chamber length of 60 mm, and angle $\beta$ was 14.82 mrad [18].

In addition, when recording EELS spectra, a necessary condition is to set the axis of the sample zone in the case of using a single-crystal substrate, which ensures a condition for the perpendicular cross-section of the sample to the incident beam.

### 1.2. Samples

The composition of NbN thin superconducting films is studied in this paper. The thickness of the NbN film on a monocrystalline sapphire substrate was 5.5 nm. Cross-sectional samples for TEM studies were prepared by cutting lamellae on a device with a focused ion beam FEI „Helios Nanolab-650“.

### 1.3. Processing of EELS spectra and interpretation of data

Samples of cross sections for conducting STEM studies made by the FIB [19] method have a thickness of $t \sim 0.8\lambda$, where $\lambda$ — the free path of electrons. This thickness of the samples avoids additional operations for deconvolution of spectra in order to eliminate the effects of multiple scattering [20].

Special attention in the processing of spectra is focused on the removal of the background component, which makes a significant contribution to the intensity of the spectrum due to the ionization of electrons at lower energy levels, the features of the detection system and the response function of the detector.

The typical spectrum of electron energy losses consists of several regions, each of which is caused by different processes of interaction of the electron beam with the atoms of the studied material. The most intense part of the spectrum, i.e. zero loss peak (ZLP) is the result of the elastic interaction of the beam electrons with the nuclei of the target atoms. The zero loss peak is used to determine the thickness of the TEM sample, and is also an important component in spectrum processing, namely, deconvolution of the spectrum in order to eliminate multiple scattering processes. The resolution of the EELS is determined by the value of the FWHM parameter for the zero loss peak, which, in turn, depends on the type of electron gun. The resolution was $\sim 0.7$ eV in this study. In practice, the zero loss peak can be asymmetric and has an extended „tail“, significantly exceeding the FWHM region. This fact should be taken into account when processing the spectrum in the region of inelastic scattered electrons, since the „tail“ contributes to the background component of the spectrum in the region of plasmon losses (in the energy range of 4–40 eV). The region of characteristic electron energy losses is in the energy range from 50 to 2000 eV, due to the Coulomb interaction between the incident electron and the electrons of the target atoms. Sharp jumps of energy losses correspond to the absorption edges of a particular element, which are superimposed on the background, to which the „tail“ from plasmon losses, lower absorption edges from other elements, multiple scattering and instrumental noise make a significant contribution.

The classical function of background subtraction in the analysis of EELS spectra is a power function of the following form

$$I_{bkg}(E) = AE^{-r}, \tag{1}$$

where $I_{bkg}$ — the number of electrons per channel in a given energy range $\delta$ near the absorption edge; $E$ — energy losses, $A$ and $r$ — constants depending on the emission current, sample thickness, detector collection angle $\beta$ and other factors. At the same time, the width of the energy interval $\delta$, in which the background component is subtracted, should exceed more than ten energy channels in magnitude and should be less than 30% of the energy of the absorption edge for the analyzed chemical element [20].

However, it is shown in Ref. [21,22] that the analysis of spectra in the region of large energy losses using a function of the form (1) does not always provide a positive result. This is attributable, firstly, to the narrow energy window

of the pre-edge region $\delta$, which affects the determination of the parameters $A$ and $r$ and significantly affects the extrapolation of the background function in the region of the absorption edge, especially if the energy window of the signal is much larger than the premarginal interval. Secondly, the premarginal region $\delta$ cannot be described by a power function, for example, in the case of overlap or close proximity of the characteristic absorption edges of different chemical elements. The following algorithms are proposed in the literature for solving the problem of drawing a background line in such situations, which are not free from shortcomings.

For example, it is proposed to use alternative models to subtract the background:
momomial exponential function

$$f(x) = ae^{bx}, \tag{2}$$

binomial

$$f(x) = ae^{xb} + ce^{dx}, \tag{3}$$

polynomial function

$$f(x) = a_n x^n + a_{n-1}x^{n-1} + \ldots + a_0, \tag{4}$$

polylogarithmic function [23]:

$$f(x) = Li_s(x). \tag{5}$$

However, it is necessary in these cases to make sure that the background subtraction is correct on samples of a known composition. It is known that the polynomial function has a significant spread when extrapolated in large energy intervals. The quantitative assessment of the correspondence of the background line to the real spectrum in the energy window $\delta$ is carried out according to the statistics of the Pearson chi-square criterion:

$$\xi^2 = \sum_i \frac{(y - y_i)^2}{y^2}, \tag{6}$$

where $y_i$ — electron counter in the $i$th channel, $y = \ln I$.

The contribution of the background component can also be taken into account within the framework of the first derivative method. This approach is implemented for detectors with parallel registration of spectra (parallel-collection EELS) [24]. Spectra shifted relative to each other by several electron volts are subtracted from one another. Such processing eliminates the slowly changing background component of the spectrum, and vice versa, the rapidly changing intensity of the absorption edge of the element manifests itself in the form of classical difference peaks, similar to the processing of Auger spectra.

Let us consider the most commonly used method of background subtraction using the dependence (1). A special algorithm is proposed in [17] for processing such spectra for the case of partial overlap of the absorption edges of various elements, when the pre-edge region cannot be used to determine the parameters $A$ and $r$ and, accordingly, to subtract the background according to the law (1). This method uses the division of the region under the spectrum into two subspaces — background and signal. The background is subtracted directly below the absorption edge as a low-order polynomial function ($n = 1$ or 2). The polynomial function is optimal for choosing the background function in the field of high electron energy losses due to the small number of parameters to be determined and the simplicity of calculation. This algorithm is suitable for spectra that do not have a sufficient energy window in front of the absorption edge of the analyzed chemical element. A significant disadvantage of this approach is the fact that the background should be described by a combination of linear functions, otherwise the algorithm does not work.

The most common method to account for background is an algorithm implemented in Gatan software Gatan Microscope Suite (GMS) for processing the EELS spectra which uses the nonlinear least-square method to calculate the power function of background subtraction. Other alternative software packages for quantitative processing of EELS spectra are also known from literature sources: EELSMODEL [25], ImageJ CSI plugin [26], automatic extraction of maps in MATLAB [27]. Each of the developed models solves its specific task in the field of electron energy loss spectroscopy.

We propose an algorithm in this paper for processing spectra that consist of overlapping absorption edges of elements, do not have a sufficient pre-edge region, and the background line for the studied chemical elements is not described by a linear function. The program code developed by us is implemented in Delphi and includes a peak analysis function, fitting symmetric peaks with the Lorentz function, removing overlapping peaks and drawing a background line according to a power law with the calculation of the parameters $A$ and $r$ included in the expression (1), by the least-square method.

The basis of the developed method of spectrum processing is the sequential removal of all undesirable „features“ in the energy range that is used to approximate the background line to the characteristic line of the studied chemical element. The assumption is used during the implementation of the sequential removal of „features“ that the integral background is described by the expression (1), and all the undesirable „features“ are described by the sum of symmetric distributions, which use Lorentz distributions.

## 2. Results and discussion

A set of single spectra was performed in the STEM mode at a separate point in the sample to implement spatial resolution when analyzing the distribution of concentrations of chemical elements in a sample at the level of fractions of a nanometer, i.e. comparable to the minimum size of an electronic probe. The spectrum acquisition time at the sample point was usually $\sim 0.5-1.5$ s and was determined by the achievement of a sufficient number of electronic

pulses in the energy loss region of interest, together with considerations on the mechanical stability of the sample position during spectrum recruitment, taking into account the hardware implementation of drift correction algorithms. The signal acquisition angle used exceeded the angle of incidence of electrons, which guaranteed the complete registration of all acts of inelastic scattering during the analysis, i.e. maximum signal collection efficiency. Single spectra were recorded in the energy range of 140–652 eV with an energy resolution of 0.5 eV.

### 2.1. Processing of a single spectrum

Figure 1 shows the initial electron loss spectrum (curve *1*), recorded in the STEM mode from a nanoscale NbN grain, which shows the lines of characteristic losses from niobium atoms Nb–$M_{4,5}$, Nb–$M_3$, Nb–$M_2$, as well as the loss line from nitrogen atoms N–K.

Since the loss spectrum in front of the niobium line Nb–$M_{4,5}$ is smooth and does not contain additional features, the energy window $A$(183–200 eV) can be directly used to subtract the background in accordance with the power dependence on energy, according to the formula (1), and the subsequent calculation of the signal from the atoms of the Nb — integral in the energy window 205–230 eV.

However, the direct application of the standard background accounting procedure to obtain an integral signal from nitrogen atoms, as can be seen from Fig. 1 curve 1, is extremely difficult due to the presence of loss lines Nb–$M_3$ and Nb–$M_2$ located in close proximity to N–K loss line.

In addition, a careful study of the curve *1* in Fig. 1 shows that even before Nb–$M_3$ and Nb–$M_2$ loss lines, an increase of the intensity is observed in the energy range from 320 to 355 eV, which prevents from defining the background by using a power-law dependence on energy. It is proposed to remove this feature from the experimental spectrum using

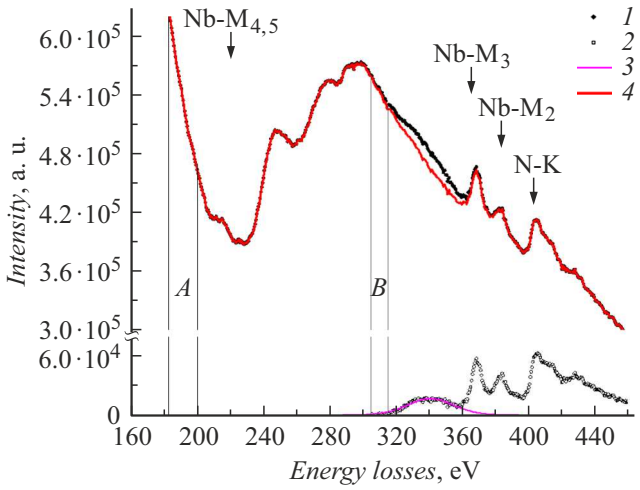


**Figure 1.** NbN electron loss spectra: *1* — initial; *2* — after subtracting the background in the window $B$; *3* — fitting the extended feature of the spectrum; *4* — after subtracting the feature *3* from the curve *1*.

the following algorithm to solve this problem. First, we select the region of the spectrum from the lower energies, where this increase in intensity has not yet been manifested, in our case — the energy window $B$ from 305 to 315 eV. We draw a background line in the energy window $B$ using the power dependence on energy according to the formula (1), after which we subtract the background from the experimental curve and get the signal shown in Fig. 1, curve *2*. A wide peak with a center at an energy of 340 eV is clearly visible in Fig. 1, curve *2*, which is defined using the fitting of the experimental curve to the calculated one in the form of a single symmetrical peak by the least-square method. We use the Lorentz distribution as symmetric peaks in this paper:

$$y(x) = c\left[1 + \left(\frac{x-d}{e}\right)^2\right]^{-f}, \qquad (7)$$

because it allows varying the shape of the peak over a wider range compared to others, for example, the Gaussian distribution, due to the shape parameter $f$, which determines the steepness of the decline of the signal when moving away from the maximum. The experimental loss spectrum has the form shown in Fig. 1, curve *4* after removal of the feature in the form of a single peak on the curve at 340 eV (Fig. 1, curve *3*).

Now, it is necessary to remove the characteristic loss lines of Nb–$M_3$ and Nb–$M_2$ from the experimental spectrum for improvement of the quality of the background acquisition while obtaining the signal from nitrogen. It is proposed in this paper to solve this task, first, by subtracting the background before Nb–$M_3$ and Nb–$M_2$ lines, then by removing these lines after performing the fitting procedure. This algorithm is implemented as follows in this paper.

An energy window $C$ in the energy loss interval from 340 to 350 eV to Nb–$M_3$ and Nb–$M_2$ lines is selected on the spectrum processed in the previous step shown in Fig. 1, curve *4* (Fig. 2, curve *1*), in which the background line is found using the standard power function according to the formula (1). The spectrum has the form shown in Fig. 2 after subtraction of the background from the curve *1* in Fig. 2, the curve *2*, which explicitly contains niobium lines requiring removal. The niobium lines of Nb–$M_3$ and Nb–$M_2$ are fitted in the energy loss range from 355 to 400 eV under three symmetric peaks, the first of which corresponds to Nb–$M_3$ line, the second peak corresponds to Nb–$M_2$ line, and the third peak describes a small plateau in the section from 390 to 400 eV (Fig. 2, curve *2*).

The fitting of the experimental spectrum to the sum of the three Lorentz (7) peaks in the region of 390 to 400 eV is performed using the nonlinear least-squares method. The use of the energy region up to the peak of energy losses for nitrogen (N–K) guarantees absence of any effect of losses from interaction with nitrogen atoms.

Next, the intensity of all three peaks is subtracted from the spectrum in Fig. 2, curve *1* after their fitting, and the energy loss spectrum has the form of the curve *3* shown in

Fig. 2. As can be seen from Fig. 2, curve *3*, the effect of Nb−$M_3$ and Nb−$M_2$ lines on the energy loss region up to the characteristic line of nitrogen is completely leveled as a result of the processing.

After that, the standard background subtraction from the transformed spectrum is performed in Fig. 2, curve *3* for the nitrogen line in the energy range from 358 to 384 eV using a power function according to the formula (1).

Fig. 3, curve *1* shows the final spectrum of the nitrogen line after the above processing in comparison with the loss line from nitrogen atoms for the GaN crystal (Fig. 3, curve *2*).

After the final processing of the spectra, a standard calculation [3] of the relative atomic concentrations of the elements (Nb and N) is performed to identify the composition of the studied niobium nitride film by integrating the spectrum of the lines of niobium (Nb−$M_{4,5}$) in the energy range from 205 to 230 eV and nitrogen (N−K) in the energy range from 392 to 417 eV. The values of the electron energy loss cross sections used in the interaction with niobium and nitrogen atoms are: $\sigma_{Nb} = 2949$ barn and $\sigma_N = 1100$ barn.

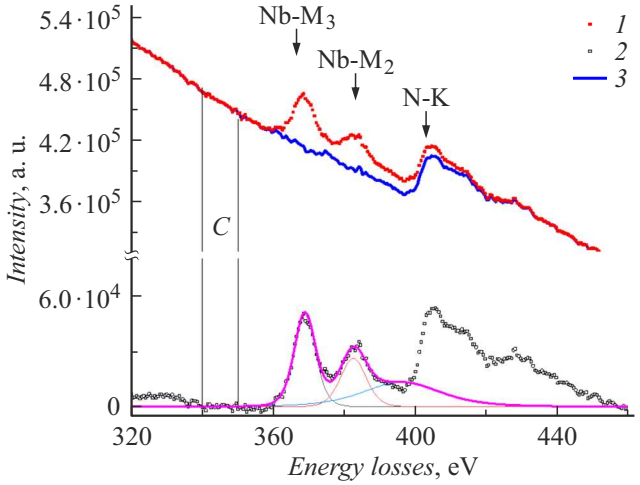


**Figure 2.** NbN electron loss spectra: *1* — after removal of the feature (Fig. 1); *2* — after subtraction of the background in the window *C*; *3* — after fitting and subtraction of Nb lines.

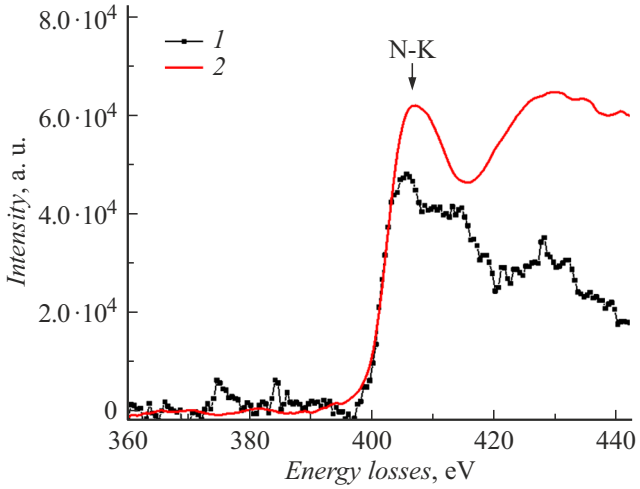


**Figure 3.** Comparison of *K*-line of nitrogen in NbN after processing *1* with nitrogen line *2* in GaN.

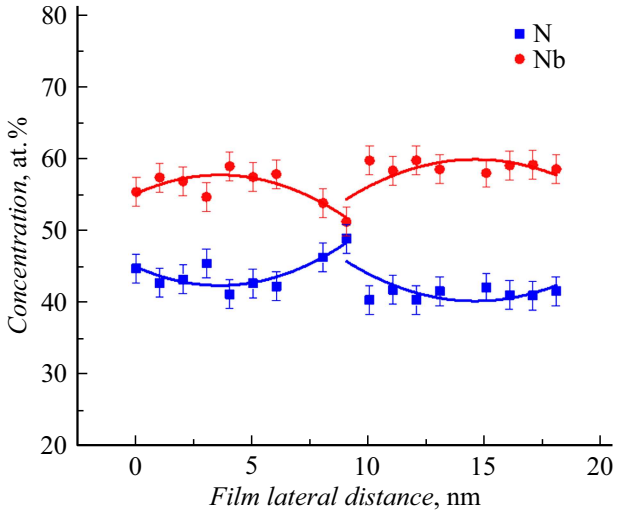


**Figure 4.** The distribution profile of the atomic concentrations of Nb and N elements along the film in the middle of its thickness.

The relative atomic concentrations of the elements are calculated using the standard ratio

$$\frac{C_N}{C_{Nb}} = \frac{I_N}{I_{Nb}} \frac{\sigma_{Nb}}{\sigma_N}. \quad (8)$$

The calculation of the relative concentrations of elements proposed in this paper, taking into account the procedure of removal of the lines of elements present in the background discrimination area before the nitrogen absorption line, was applied along a line parallel to the surface of the substrate at a depth equal to half the thickness of the film. The results of scanning along such a line are shown in Fig. 4. As can be seen from Fig. 4, the concentration profiles for both nitrogen and niobium are not completely homogeneous, they demonstrate fluctuations of concentrations with a period approximately equal to $\sim 7.5$ nm, which qualitatively corresponds to the grain size in the studied niobium nitride film. The average concentrations of chemical elements according to the results of processing of twenty points were: $C_{Nb} = (57 \pm 2)$ at.%, $C_N = (43 \pm 2)$ at.%. However, since Figure 4 shows smooth variations of concentrations with a period corresponding to the grain size, further work was performed to map concentrations over the cross-sectional area of the film.

### 2.2. Usage of the developed spectrum processing method for mapping element concentrations over the film thickness

The physical properties of nanocrystalline materials created by various deposition or sputtering methods are

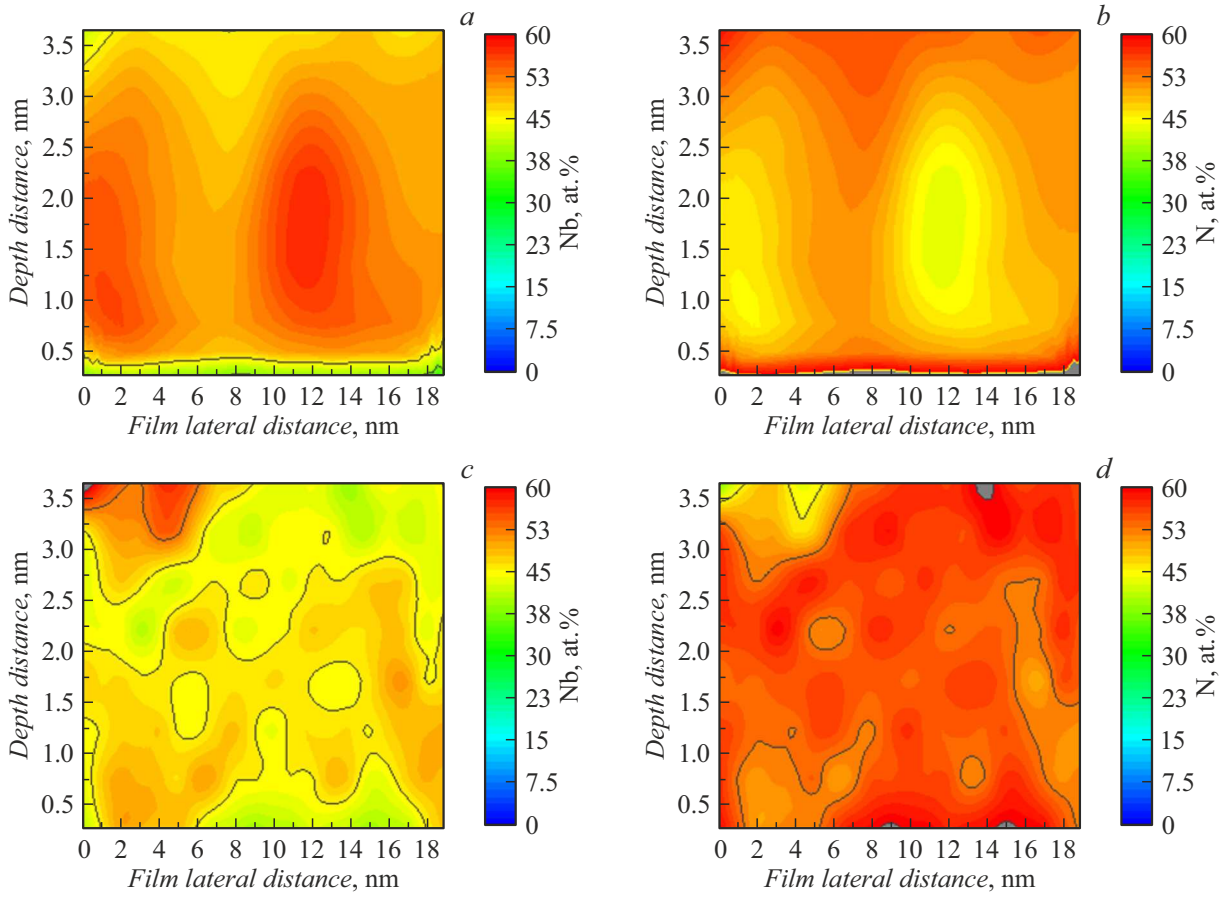


**Figure 5.** Distribution maps: *a* —niobium and *b* — nitrogen over the sample cross section, plotted using the developed method of removal of foreign lines in the area of background approximation for nitrogen; *c* — niobium and *d* — nitrogen over the sample cross-section, plotted using the standard method without removal of foreign lines in the area of background approximation for nitrogen.

determined by the distribution of chemical elements both over the coating thickness and in volume of nanocrystalline grains. There are often situations when, during the process of nucleation, grain growth or as a result of the impact of process factors, the main or impurity atoms are redistributed relative to the grain surface, as a result of which the composition of the material at the level of individual grains and in the area of grain boundaries becomes heterogeneous, which can significantly change the properties of films. Similar effects are observed not only in thin films, but also in massive materials, for example, through the formation of various kinds of segregation at grain boundaries as a result of heat treatment in the initial state [28], and as a result of radiation-induced processes. The atomic concentration distribution near grain boundaries can be visualized for both nanocrystalline and polycrystalline materials using the mapping technique which requires processing of a series of electron energy loss spectra at each point over the imaged area and subsequent construction of maps of relative concentrations of chemical elements.

By performing the above-described processing of the spectra at each mapping point, the values of the relative atomic concentrations of the elements were obtained for them, and these results were used for mapping the distribution of Nb and N chemical elements in the area of the sample which was a cross-sectional sample of a thin film of niobium nitride on a monocrystalline sapphire substrate. Since the grain size of niobium nitride is (5–6) nm, which corresponds to the thickness of the film, the microstructure of the superconducting film is a collection of niobium nitride crystallites articulated into one layer located on the surface of the substrate. The study of cross sections of such samples provides an idea of the distribution of composition at the level of individual grains and grain boundaries, which may affect their superconducting characteristics.

Figure 5 shows maps of the distribution of chemical elements over the area of the image, plotted using the developed method of spectrum processing: Figure 5, *a* — a map of the distribution of niobium atoms, and Figure 5, *b* — a map of the distribution of nitrogen atoms in comparison with the results of a similar mapping performed using a standard method, which implies drawing of a background line to discriminate the signal from the interaction of an electron beam with nitrogen atoms in the energy window from 358 to 393 eV without removal of niobium lines Nb–$M_3$ and Nb–$M_2$ (Fig. 5, *c* for Nb and Fig. 5, *d* for N).

The analysis provided on Fig. 5, *a* demonstrates that a decrease of the concentration of niobium and a decrease of the concentration of nitrogen is observed between two grains of niobium nitride, which indicates variations in the relative concentrations of elements at the grain boundaries and in the grain body. At the same time, it is obvious that suboptimal standard mapping performed by drawing a background line in an energy window containing absorption lines of another element without their removal provides a significantly larger spread of the obtained values of atomic concentrations (Fig. 5, *c, d*), it also does not allow to identify fluctuations in concentrations because of the grain structure of the studied material. Thus, it is obvious that the removal of foreign lines and features in the spectra of electron energy losses in the energy range corresponding to the background approximation window of the element under study allows both to improve measurement accuracy and to identify subtle features of atomic concentration variation when scanning along the line or by the cross-sectional area of the sample.

The plotting of such maps and their further analysis will provide additional information on the features of the superconducting properties of nanocrystalline films. Such a research method may be especially important in case of usage of ion irradiation and subsequent annealing for directional modification of the characteristics of superconducting nanowires (in particular, the transfer of a superconductor to a normal state [29]) for creation of devices based on them [30].

Figure 6 shows a TEM image with atomic resolution of a cross-section of the sample, which shows that the average grain size of niobium nitride approximately corresponds to the thickness of the film and is $\sim 5.5$ nm.

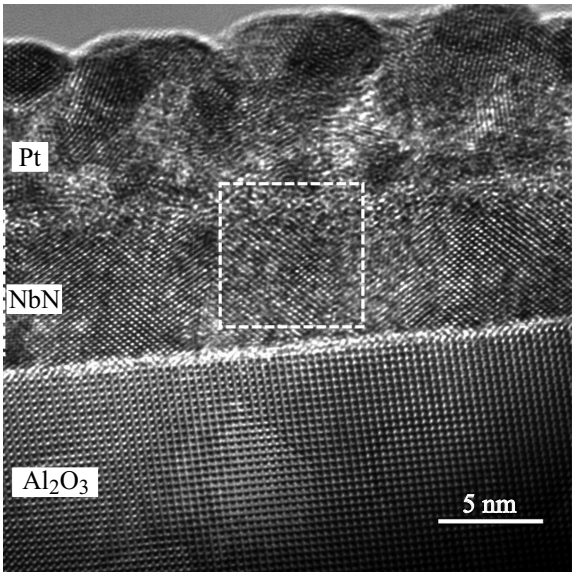


**Figure 6.** TEM image of a cross-section of a sample of polycrystalline NbN film on a monocrystalline sapphire substrate. The grain size approximately corresponds to the thickness of the film. The low contrast from the average grain is attributable to its orientation relative to the electron beam.

Thus, the developed method of eliminating the impact of closely spaced niobium lines and other features on the spectra of electron energy losses on the loss line for nitrogen atoms made it possible to reduce the spread of experimentally obtained values of atomic concentrations at various points of the sample to the level of several atomic percent.

## Conclusion

A procedure was developed to eliminate the impact of niobium characteristic lines located in the marginal region of the nitrogen characteristic line, as well as other features, on the magnitude of the signal from nitrogen atoms. The experimental NbN spectra were processed using the developed procedure. The shape of the nitrogen absorption line was compared with literary sources for verification of the correctness of the proposed method. The mapping of the distribution of chemical elements over the area of the image on cross-sectional samples of a thin film of niobium nitride on a substrate of monocrystalline sapphire was performed.

It was shown that the application of the developed method of spectrum processing makes it possible to reduce the spread of calculated atomic concentrations of elements for different points of the sample to the level of several atomic percent.

The developed method can be used for a wide class of materials in the course of conducting a local composition analysis using the EELS method in conditions when an overlap of lines of characteristic losses of various chemical elements is observed.

### Acknowledgments

The authors would like to thank V.L. Stolyarov, B.V. Goncharov, A.S. Frolov, V.N. Misko, D.A. Goncharova, E.M. Malieva for fabrication of thin films of niobium nitride and L.V. Kutuzov for fabrication of cross-section samples.

### Funding

This study was carried out under the state assignment of NRC „Kurchatov Institute“.

### Conflict of interest

The authors declare that they have no conflict of interest.

## References

[1] K.E. Prikhod'ko, M.M. Dement'eva. Crystallography Reports, **66** (4), 656 (2021). DOI: 10.1134/S1063774521040180

[2] B. Evin, E. Leroy, M. Segard, V. Paul-Boncour, S. Challet, A. Fabre, M. Latroche. J. Alloys Compd. Elsevier, **878**, 160267 (2021). DOI: 10.1016/j.jallcom.2021.160267

[3] S. Fréchard, M. Walls, M. Kociak, J.P. Chevalier, J. Henry, D. Gorse. J. Nucl. Mater., **393** (1), 102 (2009). DOI: 10.1016/j.jnucmat.2009.05.011
[4] M. Miyamoto, K. Sano, T. Sawae, M. Haruta, H. Kurata. J. Nucl. Mater. Energy, **36**, 101484 (2023). DOI: 10.1016/j.nme.2023.101484
[5] H. Ikeno, T. Mizoguchi. Microscopy, **66** (5), 305 (2017). DOI: 10.1093/jmicro/dfx033
[6] D. Bouchet, C. Colliex. Ultramicroscopy, **96** (2), 139 (2003). DOI: 10.1016/S0304-3991(02)00437-0
[7] P. Schattschneider, M. Stöger, C. Hébert, B. Jouffrey. Ultramicroscopy, **93** (2), 91 (2002). DOI: 10.1016/s0304-3991(02)00144-4
[8] S. Muto, H. Sugiyama, T. Kimura, T. Tanabe, T. Maruyama. Nucl. Instruments Methods Phys. Res. Sect. B Beam Interact. with Mater. Atoms, **218** (1−4), 117 (2004). DOI: 10.1016/j.nimb.2003.12.001
[9] N. Kawasaki, N. Sugiyama, Y. Otsuka, H. Hashimoto, M. Tsujimoto, H. Kurata, S. Isoda. Ultramicroscopy, **108** (5), 399 (2008). DOI: 10.1016/j.ultramic.2007.05.012
[10] A. Gloter, V. Badjeck, L. Bocher, N. Brun, K. March, M. Marinova, M. Tencé, M. Walls, A. Zobelli, O. Stéphan, C. Colliex. Mater. Sci. Semicond. Process, **65**, 2 (2017). DOI: 10.1016/j.mssp.2016.07.006
[11] H.L. Xin, C. Dwyer, D.A. Muller. Ultramicroscopy, 139, **38** (2014). DOI: 10.1016/j.ultramic.2014.01.006
[12] L.F. Valadares, F. Bragança, C. Silva, C.A. Leite, F. Galembeck. J. Colloid Interface Sci., **309** (1), 140 (2007). DOI: 10.1016/j.jcis.2006.12.059
[13] M.J. Mohn, J. Biskupek, Z. Lee, H. Rose, U. Kaiser. Ultramicroscopy, **219**, 113119 (2020). DOI: 10.1016/j.ultramic.2020.113119
[14] K. Kimoto, Y. Matsui. Ultramicroscopy, **96** (3−4), 335 (2003). DOI: 10.1016/s0304-3991(03)00099-8
[15] M. Horák, T. Šikola. Ultramicroscopy, **216**, 113044 (2020). DOI: 10.1016/j.ultramic.2020.113044
[16] R.F. Egerton. *Electron Energy-Loss Spectroscopy in the Electron Microscope* (Springer, NY., 2011), DOI: 10.1007/978-1-4419-9583-4
[17] S. Lu, K.J. Kormondy, A.A. Demkov, D.J. Smith. Ultramicroscopy, **195**, 25 (2018). DOI: 10.1016/j.ultramic.2018.08.013
[18] M.M. Dementieva. Avtoref. kand. diss. (SRC „Kurchatov Institute“, M., 2019) (in Russian).
[19] K.E. Prikhodko, M.M. Dementieva. ZHTF, **93** (7), 1054 (2023). DOI: 10.21883/JTF.2023.07.55.769.67-23 [K.E. Prikhodko, M.M. Dement'eva. Tech. Phys., **68** (7), 983 (2023).] DOI: 10.61011/TP.2023.07.56650.67-23]
[20] D.B. Williams, C.B. Carter. *Transmission Electron Microscopy: A Textbook for Materials Science* (Springer, NY., 2009)
[21] R.F. Egerton. Ultramicroscopy, **9** (4), 387 (1982). DOI: 10.1016/0304-3991(82)90101-2
[22] R.F. Egerton, M. Malac. Ultramicroscopy, 92 (2), 47 (2002). DOI: 10.1016/s0304-3991(01)00155-3
[23] K.L.Y. Fung, M.W. Fay, S.M. Collins, D.M. Kepaptsoglou, S.T. Skowron, Q.M. Ramasse, A.N. Khlobystov. Ultramicroscopy, **217**, 113052 (2020). DOI: 10.1016/j.ultramic.2020.113052
[24] M.M. Disko, H. Shuman. Ultramicroscopy, **20** (1−2), 43 (1986). DOI: 10.1016/0304-3991(86)90167
[25] J. Verbeeck, S. Van Aert. Ultramicroscopy, **106** (11−12), 976 (2006). DOI: 10.1016/j.ultramic.2004.06.004
[26] R. Hovden, P. Cueva, J.A. Mundy, D.A. Muller. Microscopy Today, **21** (1), 40 (2013). DOI: 10.1017/S1551929512000995
[27] C.S. Granerød, W. Zhan, Ø. Prytz. Ultramicroscopy, **184**, 39 (2018). DOI: 10.1016/j.ultramic.2017.08.006
[28] G. Dosovitskiy, V. Dubov, P. Karpyuk, P. Volkov, G. Tamulaitis, A. Borisevich, A. Vaitkevičius, K. Prikhodko, L. Kutuzov, R. Svetogorov, A. Veligzhanin, M. Korzhik. J. Luminescence, **236**, 118140 (2021). DOI: 10.1016/j.jlumin.2021.118140
[29] K.E. Prikhodko, G.Yu. Golubev. Tech. Phys. Lett., **49** (9), 8 (2023). DOI: 10.61011/TPL.2023.09.56698.19621
[30] B.A. Gurovich, K.E. Prikhodko, L.V. Kutuzov, B.V. Goncharov, D.A. Komarov, E.M. Malieva. Phys. Solid State, 64 (10), 1373 (2022). DOI: 10.21883/PSS.2022.10.54221.47HH

*Translated by A.Akhtyamov*